

SECTION V

CENTRAL STARS OF PLANETARY NEBULAE

R.H. Méndez¹²³, R.P. Kudritzki⁴ and K.P. Simon⁴

1. INTRODUCTION

This review will be concentrated on the determination of the main atmospheric parameters (T_{eff} , $\log g$, helium abundance) of PN nuclei, and of other subluminoous objects, by fitting the observed absorption line profiles with theoretical profiles obtained from non-LTE model atmosphere calculations.

The main motivations for this approach are two. The first is to be able to discuss the evolution of central stars without all the uncertainties related to the use of nebular distances; this requires to place our objects on the $\log g - \log T_{\text{eff}}$ diagram instead of the Hertzsprung-Russell diagram. The second reason is to explore the surface helium abundance of the central stars, which is likely to play an important role in a detailed discussion of their evolutionary status.

The 'model atmosphere approach' has recently become possible after extensive computations of non-LTE model atmospheres by people working in Kiel. The following selected list of references includes: (a) descriptions of the models and complementary non-LTE line formation calculations (Kudritzki, 1976; Kudritzki and Simon, 1978); (b) study of sphericity effects (Kudritzki and Simon, 1978, Gruschinske and Kudritzki, 1979); (c) application of the models to the study of massive O stars (Kudritzki, 1980), subdwarf O stars not associated with planetary nebulae (Hunger et al., 1981; Kudritzki et al., 1982a, Simon, 1982), and central stars of planetary nebulae (Méndez et al., 1981).

2. THE MODELS

The main characteristics of the models can be summarized as follows: they are plane-parallel, in hydrostatic and radiative equilibrium, computed in non-LTE for a variety of effective temperatures, surface gravities and He/H abundance ratios. No metals are included; the atmosphere is assumed to consist of H and He only. Particularly due to the assump-

tion of hydrostatic equilibrium, in a first stage we have restricted our analysis to those central stars which show predominantly absorption-line spectra. Gruschinske and Kudritzki (1979) have shown that, even for subluminous objects, it is not necessary to consider extended (spherical) hydrostatic atmospheres; in general, for the analysis of the stellar spectrum, we expect to need a significantly extended atmosphere only as a consequence of departures from hydrostatic equilibrium.

This restriction to absorption-line central stars is not so severe as it might seem at first glance, because they are quite frequent. In connection with this, we would like to remark that we have found two of the prototypes of the so-called 'continuous' objects to be absorption-line stars (NGC 3242 and NGC 7009; for the first one see Kudritzki et al., 1981). Therefore, we expect most - if not all - of these objects to be analyzable with present-day hydrostatic models.

3. COMPARISON WITH OTHER MODELS

In view of the complexity of the computer programs, it is always useful to compare the results with other work. Unfortunately, in this case there is not much overlap. In Figure 1 we have a comparison of the H_γ absorption profile computed from the hottest NLTE model of Mihalas (1972) versus the one used in the present work, for $T_{\text{eff}} = 55,000$ K, $\log g = 4$ and $y = [N(\text{He})/(N(\text{He}) + N(\text{H}))] = 0.09$. The blue wings differ because Mihalas's profile does not include the HeII absorption at 4338 Å; but the red wings are in good agreement. This was expected because the physical processes included in both models are essentially the same.

Figure 2 shows a comparison with the LTE and non-LTE H_γ profiles published by Wesemael et al. (1980) for $T_{\text{eff}} = 100,000$ K and $\log g = 6$. Here even the non-LTE models are not strictly comparable, because Wesemael et al. did not include bound-bound transitions in the statistical equilibrium equations, and considered almost pure H atmospheres. Most of the difference in Figure 2 can be attributed to these two facts. However, this statement should not be overinterpreted to mean that our models do not need improvements; both Mihalas's and our treatment of bound-bound transitions are still somewhat schematic, because in the calculation of occupation numbers, only Doppler profiles have been used, instead of fully Stark broadened profiles (of course, in the final calculation of synthetic profiles the complete broadening functions are used). Work is under way to improve the determination of occupation numbers by including Doppler and Stark broadened profiles.

4. APPLICATIONS

Although the fitting procedure is described elsewhere (see e. g. Méndez et al., 1981), we consider it worthwhile to make a few comments on the internal accuracy we can obtain. Figure 3 shows the H_γ profiles

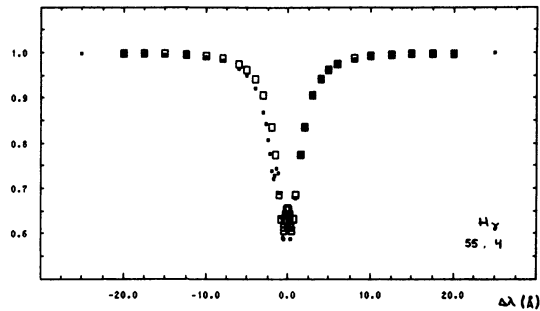


Figure 1: Comparison of H_γ theoretical absorption profiles, for $T_{\text{eff}} = 55,000$ K, $\log g = 4$ and normal He abundances. Large open squares are from Mihalas; small filled squares from Kudritzki.

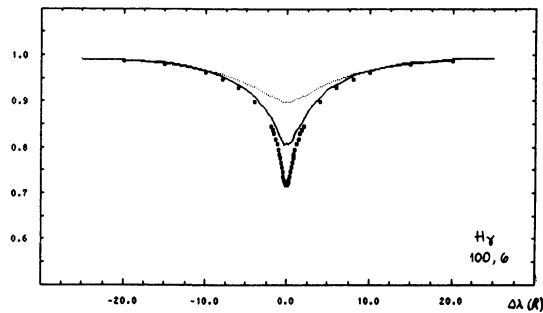


Figure 2: Comparison of H_γ theoretical absorption profiles, for $T_{\text{eff}} = 100,000$ K and $\log g = 6$. The upper (dotted) profile is from an LTE model of Wesemael et al. (1980) for $y = 10^{-6}$. The lower profile (filled squares) is from their NLTE model for the same y . The full line is from Kudritzki's model for $y = 0.01$.

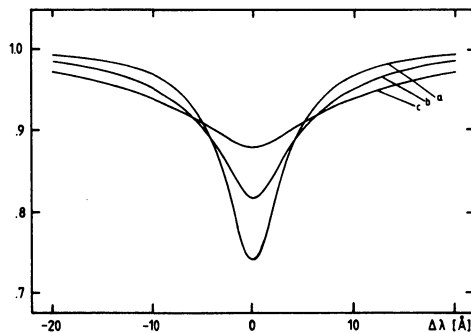


Figure 3: The variation of the theoretical H_γ profile along a curve of constant equivalent width on the $\log g - \log T_{\text{eff}}$ plane,
 a: $T_{\text{eff}} = 55,000$ K, $\log g = 5$
 b: $T_{\text{eff}} = 65,000$ K, $\log g = 6$
 c: $T_{\text{eff}} = 75,000$ K, $\log g = 7$
 These theoretical profiles (and all those in the following figures) have been convolved with a Gaussian instrumental profile having a FWHM = 3 Å, except when stated otherwise.

for three different positions on the $\log g - \log T_{\text{eff}}$ diagram. A good signal-to-noise ratio enables us to discriminate very easily between low T_{eff} , low g objects and high T_{eff} , high g ones. The situation is not so good at very low gravities; Figure 4 shows that in such cases we lose information on the temperature. One example of this problem is NGC 3242 (Kudritzki et al., 1981). The determination of T_{eff} would be much better if it were possible to use the ionization equilibrium of HeI and HeII; but in most cases the HeI lines (e.g. 4471) are too faint and/or are severely contaminated by nebular emission, and therefore provide only a lower limit for T_{eff} .

On the other hand, the determination of $\log g$ and helium abundance is quite accurate. Figure 5 shows the behaviour of HeII 4685 and HeII 4541, which yields a sensitive discrimination between low and high gravity. Figure 6 shows the effects of helium abundance. It is important to remark that the determination of $\log g$ and helium abundance is relatively insensitive to uncertainties in T_{eff} .

Our first application of the 'model atmosphere approach' to central stars of planetary nebulae (Méndez et al., 1981) was based on image-tube spectrograms obtained at the Cerro Tololo Inter-American Observatory (CTIO). More recently, we have used the SIT-Vidicon system with the R-C spectrograph of the CTIO 4-m telescope, and also the IDS with the Cassegrain spectrograph of the ESO 3.6 m telescope. A few objects were reobserved (NGC 1360, NGC 1535, Abell 36), and it was encouraging to find that three different observational techniques produce essentially the same results.

Figures 7 to 13 illustrate some of the fits we have obtained, and Table 1 gives the resulting atmospheric parameters for all the objects. Most of the earlier results (Méndez et al., 1981) remain unaffected. The exceptions are:

- (a) The Vidicon data for NGC 7293 suggest a higher temperature. This was not surprising, because our single image-tube spectrogram of this central star was not very good. It is interesting to note that this modification of the temperature did not affect our previous determination of $\log g$ and the helium abundance.
- (b) A better spectrum of NGC 4361 was obtained by adding 10 image-tube spectrograms obtained in 1981 with the R-C spectrograph of the CTIO 4-m telescope. The reductions and additions were made with the PDS microphotometer and associated software of the Kitt Peak National Observatory. The new analysis yields a somewhat smaller helium abundance than before.
- (c) The Vidicon data for NGC 1360 yield a somewhat larger helium abundance than before.

It is necessary to remark that in some cases (Abell 36, Longmore 8, Abell 15) we do not obtain a good fit. The Balmer absorption profiles suggest a temperature equal to or lower than the lower limit imposed by the absence of the HeI 4471 absorption. In such cases we have given more weight to the T_{eff} suggested by the He lines; one thing to remember is that, in cases of higher temperature, the He lower limit is not so

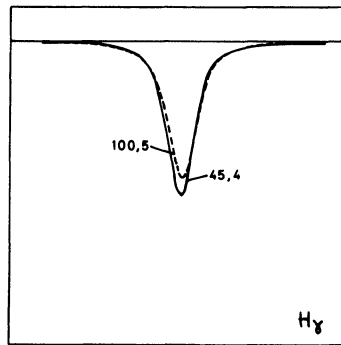


Figure 4: A comparison of H_γ profiles for $T_{\text{eff}} = 100,000$ K, $\log g = 5$, and $T_{\text{eff}} = 45,000$ K, $\log g = 4$. In both cases $y = 0.09$.

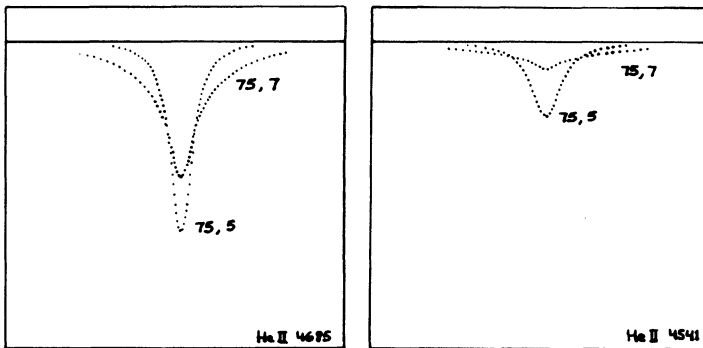


Figure 5: The effect of surface gravity on HeII 4685 and 4541, at $T_{\text{eff}} = 75,000$ K and $y = 0.09$.

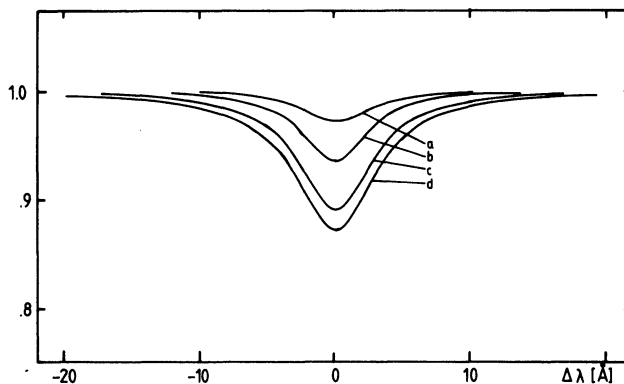


Figure 6: The effect of helium abundance on HeII 4541, at $T_{\text{eff}} = 65,000$ K and $\log g = 5$. a: $y = 0.01$, b: $y = 0.03$, c: $y = 0.09$, d: $y = 0.17$.

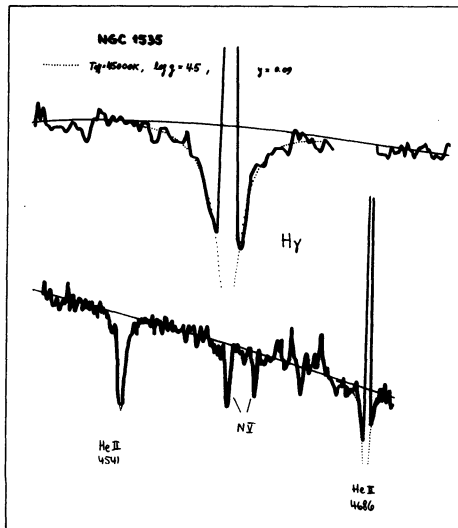


Figure 7: SIT-Vidicon line profiles of NGC 1535, fitted with non-LTE profiles convolved with FWHM = 2 Å. The results confirm an earlier analysis by Méndez et al. (1981).

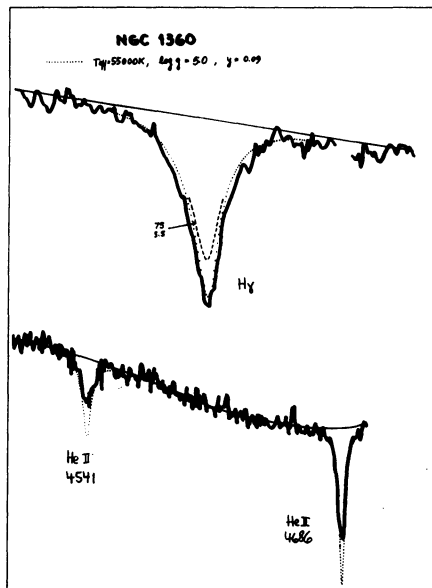


Figure 8: SIT-Vidicon line profiles of NGC 1360. The theoretical profiles are convolved with FWHM = 2 Å. The results confirm an earlier analysis by Méndez et al. (1981), except for a slightly larger helium abundance. Notice how the theoretical H γ profile for $T_{\text{eff}} = 75,000$ K fails to fit the observed profile.

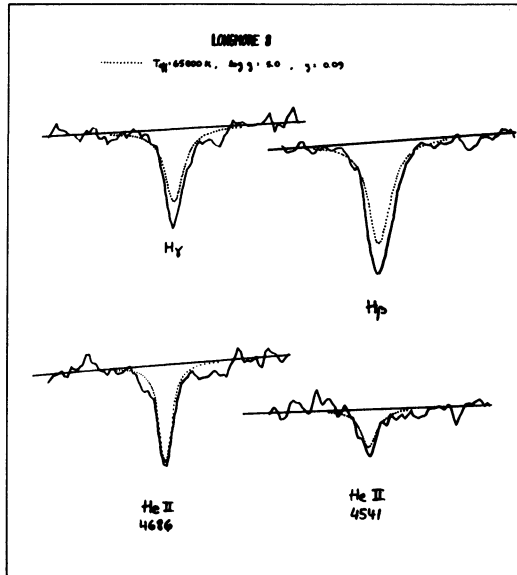


Figure 9: ESO-IDS profiles of Longmore 8. The theoretical profiles are convolved with $\text{FWHM} = 3.5 \text{ \AA}$. The Balmer absorption profiles would indicate a lower T_{eff} , which is excluded by the high helium abundance and the lack of a detectable He I absorption at 4471.

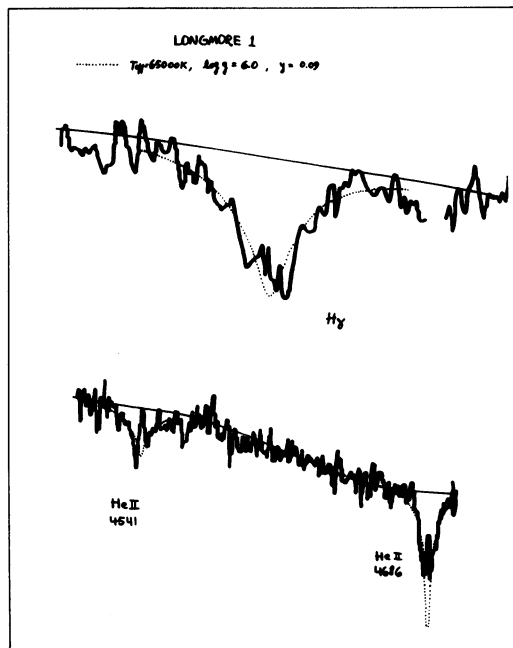


Figure 10: SIT-Vidicon line profiles of Longmore 1. The theoretical profiles are convolved with $\text{FWHM} = 2 \text{ \AA}$.

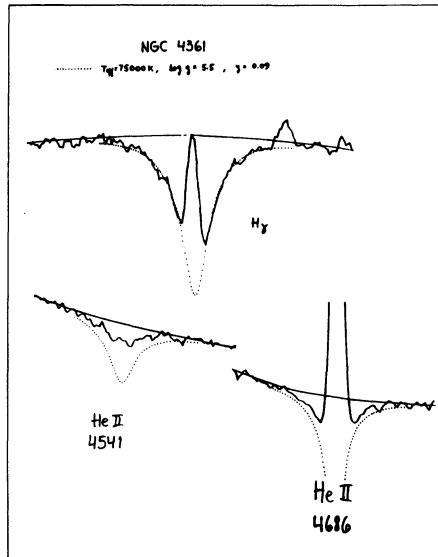


Figure 11: Absorption line profiles of NGC 4361, obtained by digitally adding 10 image-tube spectrograms taken with the CTIO 4-m R-C spectrograph. The theoretical profiles are convolved with FWHM = 3 Å. The results confirm an earlier analysis by Méndez et al. (1981), except for a slightly lower helium abundance.

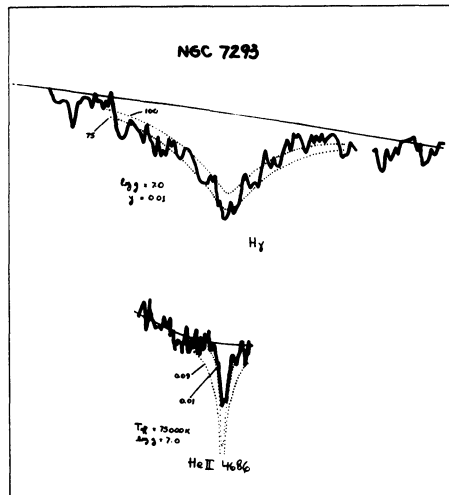


Figure 12: SIT-Vidicon line profiles of NGC 7293. The theoretical profiles are convolved with FWHM = 2 Å. The H γ profile indicates a larger T_{eff} than in the earlier analysis by Méndez et al. (1981), but $\log g$ and y remain unaffected.

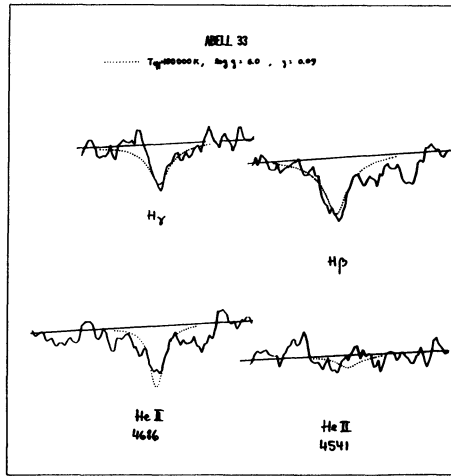


Figure 13: ESO-IDS profiles of Abell 33. The theoretical profiles are convolved with FWHM = 3.5 Å.

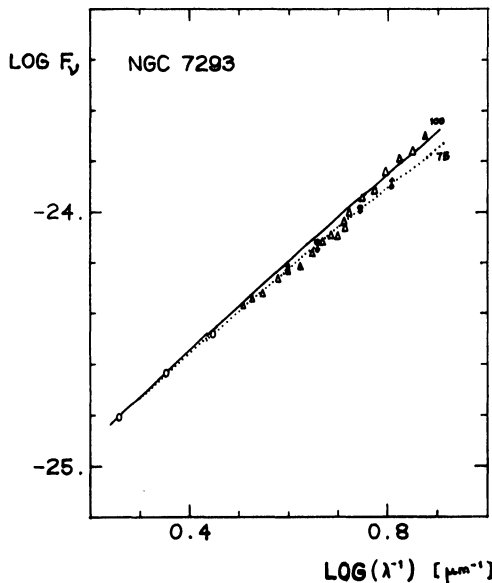


Figure 14: The 'underreddened' continuous energy distribution of the central star of NGC 7293. Open circles: Shao and Liller's (unpublished) UVB photometry. Filled circles: ANS data (Pottasch et al., 1978); the arrows indicate the corrections to the ANS fluxes applied by Bohlin et al. (1982). Triangles: IUE data (Bohlin et al., 1982). Two NLTE continuous energy distributions are plotted, for $T_{\text{eff}} = 100,000 \text{ K}$ and $75,000 \text{ K}$. In both cases $\log g = 7$ and $\xi = 0.01$.

critical, and a good fit of a Balmer line (e.g. as for NGC 4361) might well be masking a similar systematic difference, which might be as large as 20,000 K. This problem will be mentioned below in connection with the analysis of the continuous energy distributions. One final remark is that, anyway, we expect the model atmospheres to yield reliable temperature differences; in other words, we can be reasonably assured that objects like NGC 1360, Abell 36 and Longmore 8 have lower T_{eff} s than objects like Abell 33, NGC 7293 and NGC 4361.

5. THE CONTINUOUS ENERGY DISTRIBUTIONS

Once the atmospheric parameters have been determined from line profile fits, we expect the continuous energy distribution derived from the corresponding non-LTE model atmosphere to agree with the observed continuous energy distribution. This critical test has been performed in several cases of lower temperature objects, always with satisfactory results (see e.g. Kudritzki and Simon, 1978; Thé et al., 1980; Kudritzki et al., 1982a), even in the case of Of objects like Zeta Puppis (Kudritzki et al., 1982b).

What is the present situation concerning central stars of planetary nebulae? Perhaps we should start by pointing out that the T_{eff} s usually found in the literature are not directly comparable with ours, because most of them are based on comparisons with black-body energy distributions, which are well known to produce higher temperatures than model atmospheres (see e.g. Figure 13 in Méndez et al., 1981). The magnitude of this difference depends on the fitting procedure used. If the fit extends from 1500 to 6000 Å, then the difference is not larger than 15,000 K at $T_{\text{eff}} = 80,000$ K. However, if only the far UV is fitted, say from 1500 to 3000 Å, then the difference can exceed 30,000 K; i.e. a non-LTE model with $T_{\text{eff}} = 65,000$ K gives the same slope in the Balmer continuum as a black-body at 100,000 K.

It is important to emphasize that for these high-temperature objects the continuous energy distribution becomes almost insensitive to temperature, which means that a great observational accuracy is required, both for UV and for visual fluxes, and that a very good determination of the interstellar extinction is essential.

Obviously, this kind of determination was impossible before the advent of ANS and IUE. Even with these ultraviolet satellites, we are barely able to deal with this difficult observational problem; an uncertainty of $\pm 10\%$ in the absolute flux calibration can produce, even assuming a perfect visual magnitude, uncertainties of $\pm 20\%$ in T_{eff} at 100,000 K.

Let us now discuss the IUE + ANS energy distribution of the central star of NGC 7293, as shown in Figure 14. In this figure we are assuming no interstellar reddening; compare with Figure 1 of Bohlin et al. (1982), where the same data are dereddened assuming $E(B-V) = 0.012$. As stated by

them, the difference is not very large, and the precision of the slope is limited primarily by the uncertainty in the absolute calibration.

In our opinion, this continuous energy distribution does not permit an accurate determination of T_{eff} ; it cannot be fitted with any model at all. The wavelength region $\lambda > 2000 \text{ \AA}$ can be fitted with a T_{eff} slightly below 100,000 K, which is in good agreement with our T_{eff} ; but for $\lambda < 2000 \text{ \AA}$ there is an abrupt change in slope which no existing model atmosphere can reproduce. At this high temperature, the effects of line blocking are not expected to be so large. Assuming now that the quoted 10% uncertainty in the IUE fluxes can be used to rectify the energy distribution, we find a reasonable agreement with our line profile fits.

Other central stars in our sample have recently been measured with IUE, and an analysis of their continuous energy distribution has been presented in this Symposium by R.E.S. Clegg and M.J. Seaton. In a few cases the discrepancy is really large, particularly for NGC 1360 and Abell 36. According to their interpretation these two objects would be hotter than NGC 7293, in sharp contradiction with what the line profiles suggest.

Therefore, the situation appears to be rather confusing. At the present time it seems preferable to keep our minds open to all possibilities: the models may need improvements, the flux determinations also, and perhaps both are essentially correct and some objects have an ultraviolet excess. Concerning the model atmospheres, from the discussion on the line profile fits in §4 it would not be surprising to find that a slight shift is necessary in our 'temperature scale'. However, the reasonable agreement found for the energy distribution of NGC 7293 indicates that very probably some other factor is playing an important role.

6. DISCUSSION

The present (hopefully transitory) uncertainty concerning the effective temperatures of central stars makes it advisable to avoid a discussion of Zanstra temperatures; however, as stated above, surface gravities and helium abundances are well determined and deserve some comment. Figure 15 shows the positions of the 11 central stars on the $\log g - \log T_{\text{eff}}$ diagram. It is interesting to notice that the two objects with higher gravities (NGC 7293 and Abell 7), which are presumably more advanced in their evolution towards the white dwarf stage, have surface helium abundances significantly (a factor of ten) smaller than solar. This implies the action of gravitational settling and provides a very strong observational connection between these central stars and DA white dwarfs.

A complete picture of helium abundances in central stars must include those objects which appear to have little or no hydrogen in their

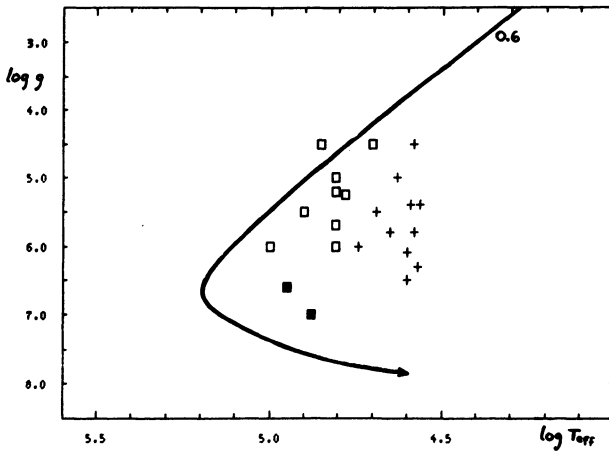


Figure 15: The $\log g - \log T_{\text{eff}}$ diagram for central stars of planetary nebulae (squares) and other hot subluminescent stars (plus signs; Hunger et al., 1981). The two filled squares correspond to Abell 7 and NGC 7293, both with $y = 0.01$. The solid line is a theoretical evolutionary track for a star of 0.6 solar masses descending from the asymptotic giant branch (Schönberner, 1981).

Table 1

ATMOSPHERIC PARAMETERS OF CENTRAL STARS

OBJECT	T_{eff}	$\log g$	$y = \frac{N(\text{He})}{N(\text{He}) + N(\text{H})}$
NGC 1360	60 $\begin{smallmatrix} +15 \\ -5 \end{smallmatrix}$	5.2 ± 0.2	0.06 ± 0.03
NGC 1535	50 $\begin{smallmatrix} +10 \\ -5 \end{smallmatrix}$	4.5 ± 0.3	0.09 ± 0.03
NGC 3242	70 $\begin{smallmatrix} +30 \\ -20 \end{smallmatrix}$	4.5 ± 0.5	0.10 ± 0.03
NGC 4361	80 ± 10	5.5 ± 0.3	0.05 ± 0.02
NGC 7293	90 ± 10	6.6 ± 0.3	$0.01 \begin{smallmatrix} +0.01 \\ -0.005 \end{smallmatrix}$
Abell 7	75 ± 10	7.0 ± 0.5	0.01 ± 0.005
Abell 15	65 ± 10	6.0 ± 0.5	0.09 ± 0.04
Abell 33	100 ± 30	6.0 ± 0.5	0.09 ± 0.05
Abell 36	65 ± 10	5.2 ± 0.3	0.13 ± 0.04
Longmore 1	65 ± 10	5.7 ± 0.3	0.10 ± 0.03
Longmore 8	65 ± 10	5.0 ± 0.5	0.11 ± 0.03

spectra: the WC central stars (for a recent reclassification see Méndez and Niemela, 1982) and several objects with predominantly absorption line spectra, e.g. NGC 246, K 1-27, Longmore 3 and Longmore 4 (Méndez and Kudritzki, in preparation). Several authors have pointed out that these objects may be likely progenitors of non-DA white dwarfs. Unfortunately, non-LTE model atmosphere analyses of these objects are not yet possible.

From the non-LTE analyses already performed, it appears reasonable to suggest that the time scale for helium depletion in hydrogen-dominated atmospheres of PN central stars is comparable to or shorter than the time scale for nebular dissipation. A better determination of this time scale from a more numerous sample may help to put constraints on theoretical models of post-AGB (asymptotic giant branch) evolution.

It is also of interest to compare the positions of PN central stars in Figure 15 with the positions of 11 hot subluminous stars not associated with planetary nebulae (Hunger et al., 1981). The clean separation obtained cannot be affected by uncertainties in T_{eff} , or (obviously) in the distances, and is a strong argument favoring the assignment of systematically lower masses to the hot subluminous stars not associated with PN. This hint may lead to some clarification of the late stages in the evolution of low-mass stars. A reasonable working hypothesis (Hunger and Kudritzki, 1981) is to interpret the non-PN hot subdwarfs as stars which are not able to reach the asymptotic giant branch, and evolve directly from the horizontal branch towards the white dwarf stage, providing the lower-mass end of the white-dwarf mass distribution.

REFERENCES

- Bohlin, R.C., Harrington, J.P., Stecher, T.P. 1982, *Astrophys. J.* 252, 635.
- Gruschinske, J., Kudritzki, R.P. 1979, *Astron. Astrophys.* 77, 341.
- Hunger, K., Gruschinske, J., Kudritzki, R.P., Simon, K.P. 1981, *Astron. Astrophys.* 95, 244.
- Hunger, K., Kudritzki, R.P. 1981, *The ESO Messenger*, No. 24, p. 7.
- Kudritzki, R.P. 1976, *Astron. Astrophys.* 52, 11.
- Kudritzki, R.P. 1980, *Astron. Astrophys.* 85, 174.
- Kudritzki, R.P., Méndez, R.H., Simon, K.P. 1981, *Astron. Astrophys.* 99, L15.
- Kudritzki, R.P., Simon, K.P. 1978, *Astron. Astrophys.* 70, 653.
- Kudritzki, R.P., Simon, K.P., Hamann, W.R. 1982b, submitted to *Astron. Astrophys.*
- Kudritzki, R.P., Simon, K.P., Lynas-Gray, A.E., Kilkenny, D., Hill, P.W. 1982a, *Astron. Astrophys.* 106, 254.
- Méndez, R.H., Kudritzki, R.P., Gruschinske, J., Simon, K.P. 1981, *Astron. Astrophys.* 101, 323.
- Méndez, R.H., Niemela, V.S. 1982, in *IAU Symp.* 99.
- Mihalas, D. 1972, *NCAR Tech. Note* TN/STR-76.

- Pottasch, S.R., Wesselius, P.R., Wu, C.-C., Fieten, H., van Duinen, R.J. 1978, *Astron. Astrophys.* 62, 95.
- Schönberner, D. 1981, *Astron. Astrophys.* 103, 119.
- Simon, K.P. 1982, *Astron. Astrophys.* 107, 313.
- Thé, P.S., Tjin A Djie, H.R.E., Kudritzki, R.P. and Wesselius, P.R. 1980, *Astron. Astrophys.* 91, 360.
- Wesemael, F., Auer, L.H., Van Horn, H.M., Savedoff, M.P. 1980, *Astrophys. J. Suppl. Ser.* 43, 159.

* Based partly on observations made at the ESO, La Silla, Chile

¹ Instituto de Astronomia y Física del Espacio, C.C. 67, Suc. 28, 1428 Buenos Aires, Argentina

² Visiting Astronomer, Cerro Tololo Inter-American Observatory, operated by the Association of Universities for Research in Astronomy, Inc., under contract with the U.S. National Science Foundation

³ Member of the "Carrera del Investigador Científico", Conicet, Argentina

⁴ Institut für Astronomie und Astrophysik der Universität München, Scheinerstr. 1, D-8000 München 80, Federal Republic of Germany

MATHIS: What do you think the effects of line blanketing would be in the IUE spectral region, and what would be the effects of a stellar wind on the models?

MÉNDEZ: Concerning line blanketing, I hardly dare to make a prediction, although perhaps we should not expect a large effect. I would certainly like to see models incorporating line blanketing!

As to the second part of your question, some of these stars have winds, but we have restricted our analysis to those objects showing predominantly absorption lines and have used lines which are formed rather deep in the photosphere. Therefore, we do not expect the wind, when present, to affect our results significantly. The situation changes when there is a velocity field deep in the photosphere. Probably for the Of and Ofp central stars, and certainly for WC central stars, we need hydrodynamic models of extended atmospheres which, of course, are not yet available.

HEAP: Have you determined the N or C abundances in any of these stars?

MÉNDEZ: Not yet. Some analysis of resonance ultraviolet lines in the spectra of sdO stars has been done at Kiel. We have IUE high dispersion spectra of a few central stars, but their study has just started.

- HARRINGTON: Since you showed our plot of the ultraviolet data for NGC 7293, I think I should comment on the Zanstra temperatures we found (Bohlin, Harrington and Stecher, 1982, Ap. J. 252, 635): $T_Z(\text{H I}) = 100\ 000\ \text{K}$ and $T_Z(\text{He II}) = 123\ 000\ \text{K}$. In deriving $T_Z(\text{He II})$, we assumed a normal helium abundance. With the low helium abundance which you find, $T_Z(\text{He II})$ will surely be below 123 000 K, perhaps close to the value of 100 000 K which you derive from the line profiles.
- CLEGG: I wish to draw attention to a result derived from IUE data and reported by several people at the second poster session. Hot sub-dwarf O stars often show a flux, for $\lambda < 1500\ \text{\AA}$, in excess of black-body or NLTE model atmosphere predictions. NGC 1360 is the best example. Although the IUE flux calibration is a little (perhaps 15%) uncertain in this spectral region, the effect seems to be quite real.
- MÉNDEZ: Yes, this discrepancy appears to be serious. A comparison of observed line profiles indicates that objects like NGC 1360 and A 36 have lower temperatures than, e.g. NGC 7293, in contradiction with what is suggested by the observed (IUE) continuous energy distributions.
- CLEGG: The problem is that the line blanketing should be treated in NLTE - but this is impossible for 92 elements, each with many ions and energy levels! The problem could be tackled in LTE (although much atomic data is missing), but to consider all lines as being formed in pure absorption would lead to erroneous model temperature structures.
- LYNAS-GRAY: What is the interpretation of low helium abundances in two high gravity stars? For sdO stars, the distinction between high and low helium abundance is at $T_{\text{eff}} \approx 40\ 000\ \text{K}$.
- MÉNDEZ: Both for sdO's and for PN nuclei, the most probable explanation would appear to be gravitational settling. However, the detailed mechanisms at work in each case may differ and the internal structures almost certainly differ. These problems are essentially unsolved at the present time.
- RENZINI: How can you distinguish a sdO star from a PN nucleus whose nebula has already dispersed?
- MÉNDEZ: The sdO's and PN nuclei do not overlap on the $\log g / \log T_{\text{eff}}$ diagram, and it seems that sdO's cannot be explained as post-AGB objects. We still have no quantitative information on the gravities of the lower temperature central stars because most of them have Ofp or WC spectra, but we would expect all low T_{eff} central stars to have much lower gravities than most of the sdO stars not associated with PN.
- WEIDEMANN: In this connection, the separation of the locations of the sdO's and the nuclei of PN in the $\log g / T_{\text{eff}}$ diagram (Hunger et al., 1981, Astron. Astrophys.; Méndez et al., 1981, Astron. Astrophys.) is evidently due to the fact that sdO's have masses smaller than $0.55 M_{\odot}$, as would be expected from stellar evolutionary calculations which show that, e.g. horizontal branch stars less massive than $0.55 M_{\odot}$ do not go up to the AGB but move over directly to the White Dwarf region.